

The following scientific article was officially published in the journal *Computerized Medical Imaging and Graphics*. This article's citation is as follows:

Harmouche, Rola, Farida Cheriet, Hubert Labelle, and Jean Dansereau. "3D registration of MR and X-ray spine images using an articulated model." *Computerized Medical Imaging and Graphics*, vol. 36, no. 5 (2012): pp. 410-418.

**doi:** [10.1016/j.compmedimag.2012.03.003](https://doi.org/10.1016/j.compmedimag.2012.03.003)

The manuscript, as accepted by the publisher, is reproduced here, as it appears in the first author's Ph.D. thesis, entitled *Fusion multimodale d'images pour la reconstruction et la modélisation géométrique 3d du tronc humain*. The thesis citation is as follows:

Harmouche, Rola. "Fusion multimodale d'images pour la reconstruction et la modélisation géométrique 3D du tronc humain." PhD diss., École Polytechnique de Montréal, 2012.



**Rola Harmouche, 2012**

© 2012 Rola Harmouche. This work is licensed under the Creative Commons Attribution-NonCommercial-NoDerivatives 4.0 International License. To view a copy of this license, visit:

<http://creativecommons.org/licenses/by-nc-nd/4.0/>

## CHAPITRE 4 : Article : Fast 3D registration of MR/X-ray spine images using an Articulated mode

Rola Harmouche<sup>1</sup>, Farida Cheriet<sup>1,2</sup>, Hubert Labelle<sup>2</sup>, Jean Dansereau<sup>1</sup>

1 : École Polytechnique de Montréal. 2500, chemin de Polytechnique, Montréal, H3T 1J4

2 : Hôpital Ste-Justine, 3175, Chemin de la Côte-Sainte-Catherine, Montréal H3T 1C5

### 4.1 Présentation

Cet article a été publié dans le journal : Computerised medical imaging and graphics (CMIG). Le but de cet article est de recalibrer les vertèbres extraites à partir d'images RM avec des vertèbres extraites à partir d'images RX pour des patients scoliotiques, en tenant compte des déformations non-rigides due au changement de posture entre ces deux modalités. À ces fins, une méthode de recalage à l'aide d'un modèle articulé est proposée. Cette méthode a été comparée avec un recalage rigide en calculant l'erreur sur des points de repère, ainsi qu'en calculant la différence entre l'angle de Cobb avant et après recalage. Une validation additionnelle de la méthode de recalage présentée ici se trouve dans l'annexe A. Ce travail servira de première étape dans la fusion des images RM, RX et TP du tronc complet. Donc, cet article vérifie l'hypothèse 1 décrite dans la section 3.2.1.

### 4.2 Abstract

This paper presents a magnetic resonance image (MRI)/X-ray spine registration method that compensates for the change in the curvature of the spine between standing and prone positions for scoliotic patients. MRIs in prone position and X-rays in standing position are acquired for 14 patients with scoliosis. The 3D reconstructions of the spine are then aligned using an articulated model which calculates intervertebral transformations. Results show significant decrease in registration error when the proposed articulated model is compared with rigid registration. The method can be used as a basis for full body MRI/X-ray registration incorporating soft tissues for surgical simulation.

### 4.3 Introduction

Idiopathic scoliosis is a disease of unknown cause characterized by a complex three-dimensional curvature of the spine with onset most often discovered during puberty [2]. Scoliosis affects 5.1% of adolescent girls and 3.5% of adolescent boys, with the more severe cases requiring treatment being

girls [3]. Curvature measures are usually obtained from standing X-rays on which the skeletal structures are visible. The spinal deviation in turn affects the external appearance of a scoliotic patient, which is usually characterized by a lateral trunk asymmetry and or a rib hump. Such external deformations are often aesthetically undesirable for patients and can cause psychological problems. In more severe cases, the spinal curvature can affect the physical functioning of the patient with symptoms such as chronic back problems or pulmonary problems [4]. For less severe cases, a brace can be worn in order to limit the progression of the spinal deformation. When the spinal curvature is very pronounced surgery is necessary in order to correct some of the undesirable deformation. However, the effects of treatment on the external shape of the trunk cannot be predicted prior to treatment completion. A simulator was recently developed using physical models in order to simulate the effects of treatment on the external shape of the trunk [7]. Promising results were obtained, though tissue characteristics were empirically modeled due to lack of patient-specific information. A complete model of the patient trunk, which would incorporate both spine and soft tissue information, would allow for a more precise propagation of the surgical correction from the spine to the external shape of the trunk. This can lead to a better prediction of the surgical outcome. Such a model would require fusion of soft tissue information, typically obtained from MRIs in prone position, and spine information, typically obtained from X-rays in standing position. Spine information is extracted from X-rays for several reasons : Although vertebral bodies can be extracted from MRI data, low image resolution does not allow for proper localization of pedicles. In addition, soft tissues from MRI data will only be acquired for a generic model, as they are not part of the clinical protocol for pre-surgical scoliosis patients due to prolonged acquisition times. X-rays on the other hand are routinely acquired. Finally, a patient-specific model of the spine is required in standing position as this would reflect the true extent of the curvature of the spine. A representation of the spine in standing position is only available from X-ray images. Thus, this paper registers MRI and X-ray spine images of scoliotic patients in order to compensate for the postural differences, as a first step towards full body registration.

### **4.3.1 Related Work**

Previous works on on MRI/X-ray registration were applied to interventional imaging [84, 85, 86], angiographic imaging [87, 88, 89, 90, 91, 92, 93], cerebral[93, 94, 86, 95], cardiac and cardiovascular imaging[96, 97, 98, 99, 100, 101], and several other fields [102, 103, 104, 105, 106, 107]. A detailed review of MRI/X-ray and other 2D/3D registration techniques can be found in [108]. Methodologies used in such applications cannot be directly applied to registration of the spine due to the difference in stiffness characteristics between the vertebrae and the anatomical structures studied in the above mentioned works.

Considerably less work has been done on MRI/X-ray registration of the spine in particular. Van

de Kraats et al. [34] registered MRI to X-ray data using fiducials manually placed on cadaveric data. The placement of fiducials is not realistic in real patient data. Tomazevic et al. [109] rigidly registered 2D X-ray images to CT and MRI data of lumbar vertebrae obtained from a cadaver. They used a novel criterion function in order to evaluate a match between normals to the surface and corresponding back-projected intensity gradients of X-ray images. Fiducials considered as a gold standard were used for validation purposes. The method assumed that surfaces of bony structures were extracted preoperatively from CT or MR images. In later work [35], they used a novel similarity measure based on mutual information in order to rigidly register a series of 2D X-ray images to CT and MRI data. Although as little as 1 X-ray image was used for X-ray/CT registration, 9 X-ray images were required per patient for X-ray/MRI registration, which is not possible to acquire in normal clinical settings due to radiation issues. Van de Kraats et al. [110] used multispectral MRI in order to generate CT-like data for rigid registration of cadaveric vertebral bodies with X-ray images. A mapping function from MR to simulated CT was obtained using training data. Results showed an improvement when compared to direct use of MRI data. Markelj et al. [111, 112] used as little as 2 2D X-rays in order to perform rigid MRI/X-ray registration on the same data as in [110]. They did so by matching 3D gradients of 3D images to 3D gradients coarsely reconstructed from 2D X-ray images. The advantage of this method is that it did not require segmentation.

The difference in posture between the standing position in which the X-rays are acquired and the prone position in which the MRIs are acquired, which has been demonstrated in [38], causes a non-linear deformation in the shape of the spine between the two image modalities being registered. Thus, purely rigid registration techniques are not applicable as they are unable to compensate for this change in posture. Furthermore, with the knowledge that the vertebrae themselves are rigid structures, non-rigid registration algorithms might deform them in a manner that does not reflect their physical properties, and are thus unsuitable for the current application. For example, we have previously shown how a thin-plate splines registration of a vertebra erroneously changes its shape [113]. In order to take into account the rigid nature of vertebrae and the non-rigid deformations that occur in the spine, Little et al. [41] registered 2D MRI images of the head and neck of the same patient in two different postures by registering soft tissue using modified thin-plate splines. The modified thin-plate spline formulation allowed segmented vertebral structures to be constrained to rigid deformations by setting the non-rigid component to 0. Similar work was done by Rohr [42], requiring only a few corresponding points instead of full segmentation of the rigid structures. These methods did not however register MRI and X-ray data, nor did they model the deformations that are due to differences in posture. Our team has recently developed an articulated model representation for the spine using X-ray data but did not use it for registration purposes [73]. This model was used by Kadoury et al. [76] in order to register a preoperative reconstructed X-ray personalized model to the intraoperative CT data of a scoliotic surgical patient. The work in [76] optimized an

energy function using Markov random fields which required significant computation time. Such a model, consisting exclusively of vertebral information, did not provide soft tissue information. In addition, acquiring CT scans for the entire trunk of a patient is not feasible due to radiation issues. MR images on the other hand are non-invasive and contain soft tissue information required to build a more complete patient model which can be useful for surgical planning.

### 4.3.2 Overview of the method

This paper proposes the use of articulated models for a three dimensional registration of the spine using X-ray reconstructions in standing position and MRI 3D reconstructions in supine position to compensate for the effect of postural differences on the curvature of the spine. Taking into account the vertebrae's physical characteristics, they are modeled as rigid bodies, and inter-vertebral rigid transformations are calculated using local vertebral coordinate systems. The overall transformation between the vertebrae extracted from the two image modalities is calculated by finding the transformation between world coordinates and the vertebrae's local coordinate systems. The method is fast since a closed form solution is obtained, thus requiring no optimization in the registration process, as will be seen in the results section. The methodology and preliminary results have been presented in [113] with only five patients. In the present work, the proposed method is compared to rigid registration using 14 patients with scoliosis and the target registration error between landmarks is calculated. The additional patient data also allows us to perform a more elaborate validation. The variability of manual MRI landmark localization is assessed by comparing two manual landmark localizations for each of seven patients. Also, in order to provide more clinically significant results, Cobb angles are calculated for each patient before and after registration using our proposed method and compared to rigid registration. Finally, the shape of the spine is analyzed in standing and supine postures using average Cobb angles over the entire dataset. In addition, average spine models for the MRI and X-ray data are compared using statistical model analysis in order to show general curvature differences. Such an analysis sheds light onto the postural corrections required for registration, and can be useful during surgical planning.

This article is organized as follows : Section 4.4 describes the proposed articulated model registration framework, the experimental setup, and the methods used to validate our work. The results of the proposed method are shown in section 5.5, followed by a conclusion in section 5.6.

## 4.4 Materials and methods

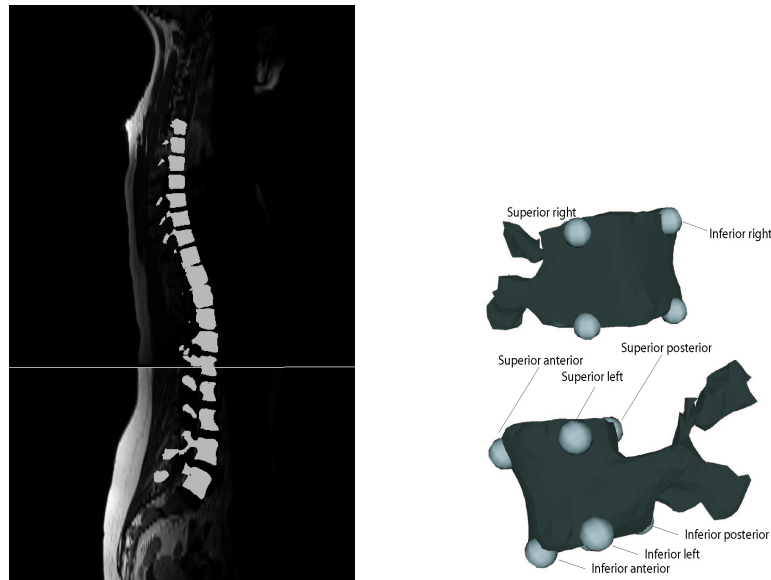
In this section, the methodology used for the registration is outlined. First, MRI and X-ray data are acquired and the vertebrae are reconstructed in 3D (section 4.4.1). Then, an articulated model is obtained by calculating local inter-vertebral transformations. This model is used for the

registration of the X-ray and MRI spine model (section 4.4.2). Finally, the validation methods are presented (section 4.4.3). First, the target registration error and Cobb angle measurements are used in order to evaluate the proposed registration framework. Then, an analysis of the shape of the spine in standing and supine postures is performed using Cobb angle measurements and average spine models.

#### 4.4.1 Data acquisition

MRI and X-ray data available at Ste-Justine hospital in Montreal from 14 patients with scoliosis and awaiting surgery were used for this study (average postero-anterior Cobb angle in standing position is 45.99 for the thoracic area and 44.51 for the lumbar area). In order to generate a 3D model of the spine from MRI data, T1-weighted MRI images are acquired using a Siemens Symphony system (1.5 Tesla, TR/TE = 771/15, 704x704, 350 FOV). Sagittal slices of 0.5mm by 0.5mm in-plane resolution and 3mm thickness are acquired with a 3.6mm separation between slices. The 3D shape of the seventeen thoracic and lumbar vertebrae is manually segmented from these images (figure 4.1(a)) and eight landmark points are manually labelled on each vertebra using TomoVision's SliceOmatic software. These eight landmarks per vertebra will be used to generate the articulated model. For all MRI data, landmarks are placed on the left, right, posterior and anterior corners of the inferior and superior end plates of the vertebral body for all thoracic and lumbar vertebrae (figure 4.1(a)). Landmarks were chosen to be on the vertebral bodies as the pedicles are more difficult to distinguish on the MRI due to the resolution.

In order to generate a 3D model of the spine for a patient from X-ray data, six landmarks manually identified on each vertebra by experts on both biplanar radiographs (Postero-anterior and lateral) are used to generate 3D landmark points representing the vertebral column. The directions of the radiographs were chosen to optimize the reconstruction process [15]. The landmarks are placed on the centers of the superior and inferior plates of the vertebral bodies, and below and above the left and right pedicles. These landmarks are consistently chosen for X-rays at Ste-Justine Hospital due to good landmark visibility [114]. The 3D position of the points is obtained using a stereoradiography 3D reconstruction method [15]. The obtained landmarks are used to map a generic vertebral dictionary onto the patient space using free-form deformations. The dictionary consists of a geometric representation of vertebral surfaces obtained from a cadaveric specimen [115]. For all X-ray data, the same six landmarks that are used in order to generate the 3D vertebral model are also used in order to generate the articulated model. The method thus allows the flexibility of using different landmarks on each modality and can be adapted for use without manual intervention, provided automatic vertebral segmentation methods are applied.



(a) MRI image and extracted vertebrae (b) Landmarks on vertebrae

Figure 4.1 3D reconstruction of vertebrae from MRI sagittal slices along with manually labeled landmarks on each of the vertebrae.

#### 4.4.2 Articulated model registration

The vertebrae reconstructed from the MRI data are aligned with those of the X-ray data using the articulated model proposed by Boisvert et al. [73], which models the spine as a series of local inter-vertebral rigid transformations (figure 4.2). First, for each patient, the intervertebral transformations are computed for each of the vertebrae for the MRI and X-ray data separately. In order to calculate the inter-vertebral transformation  $T_{i,i+1}$  from vertebra  $V_i$  to the consecutive vertebra  $V_{i+1}$ , a local coordinate system is defined for each vertebra using the landmarks obtained in the previous section and in the following manner : The 3D coordinates of landmarks on each vertebra are used to find the center of the local vertebral coordinate system. The z-axis is defined as passing through the center from inferior to the superior end of the vertebra, the y-axis from left to right, and the x-axis from posterior to anterior. The Gram Schmidt algorithm is then used to construct an orthogonal basis from these axis forming the local coordinate systems. The intervertebral transformation matrices are then calculated as rigid transformations between the local coordinate systems of two consecutive vertebrae. The position and orientation of the first vertebra is defined using the transformation between the absolute world coordinate system and the first vertebra's local coordinate system ( $T_{0,1}$ ).

Second, the overall transformation  $T_{0,i}$  between the world coordinates and the  $i$ th vertebra for the MRI ( $T_{0,i_{MRI}}$ ) and the X-ray ( $T_{0,i_{X-ray}}$ ) can be defined as the composition of the local inter-

vertebral transformations with the global transformation of the first vertebra in the following manner :

$$\begin{aligned} T_{0,i_{MRI}} &= T_{i-1,i_{MRI}} \circ T_{i-2,i-1_{MRI}} \circ T_{i-3,i-2_{MRI}} \circ \dots \circ T_{1,2_{MRI}} \circ T_{0,1_{MRI}}, \\ T_{0,i_{X-ray}} &= T_{i-1,i_{X-ray}} \circ T_{i-2,i-1_{X-ray}} \circ T_{i-3,i-2_{X-ray}} \circ \dots \circ T_{1,2_{X-ray}} \circ T_{0,1_{X-ray}}. \end{aligned} \quad (4.1)$$

In practice, for the sake of simplicity, we calculated one overall transformation per vertebra by obtaining the rigid transformation between the absolute world coordinate system and the local coordinate system of each of the vertebrae directly. This also avoids the accumulation of errors caused by the multiplication of numerous local transformations. Finally, in order to register any vertebra  $i$  on the MRI image  $V_{i-MRI}$  to its corresponding vertebra on the X-ray data  $V_{i-X-ray}$ , the inverse of the transformation from the absolute world coordinates  $T_{0,i_{MRI}}$  is first applied, followed by the transformation from absolute world coordinates to  $V_{i-X-ray}$  :

$$T_{i-MRI-X-ray} = T_{0,i_{X-ray}} \circ T_{0,i_{MRI}}^{-1}. \quad (4.2)$$

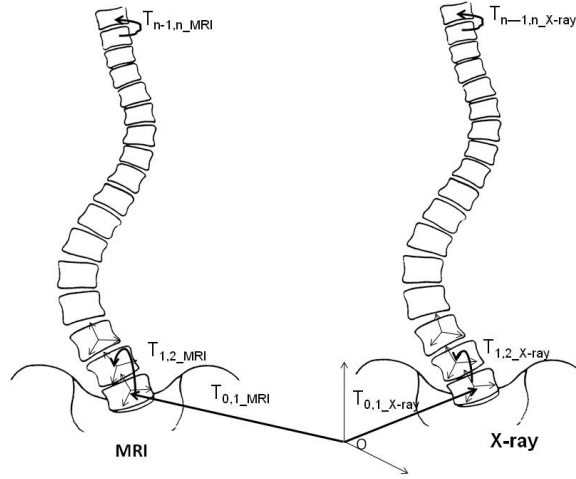


Figure 4.2 Local and global transformations forming the articulated model required to align MRI onto X-ray vertebrae. The local transformations are defined from vertebra  $V_i$  to the consecutive vertebra  $V_{i+1}$ . The global transformation from world coordinates to the first vertebra is defined as  $T_{0,i}$



### 4.4.3 Validation

#### Registration error

In order to provide a quantitative validation of the registration method, corresponding points are obtained from the MRI and X-ray vertebrae. Since the 6 landmarks per vertebra extracted from the X-ray data for registration purposes are different from the 8 landmarks per vertebra extracted from the MRI data, points corresponding to the 8 landmarks per vertebra extracted from the MRI data are inferred from the X-ray reconstructions. Rigid registration is performed by minimizing the least squares distance, using the method in [116] as implemented in the Visualization toolkit by Kitware (<http://www.vtk.org/>). Half of the 8 landmarks per vertebra that are extracted from the MRI and X-ray data for validation purposes are used for the rigid registration, resulting in 68 landmarks per patient over the entire spine. The remaining half of the corresponding points is used to calculate the target registration error (TRE) for both our proposed articulated model method and rigid registration for the lumbar and thoracic portions of the spine. The TRE is defined as the Euclidean distance in mm between the X-ray and registered MRI corresponding points. This is done in order to verify whether this error is decreased when using the proposed method thus signifying better alignment. Errors are reported for the thoracic and the lumbar parts of the spine separately in order to assess in which part our proposed method brings the greatest improvement.

Also, in order to provide more clinically meaningful results, the degree of the curvature of the spine is measured on the reconstructed data using Cobb angles [117] for the thoracic and lumbar areas separately. This angle is measured between 2 inflection points of the vertebral column. The intersecting lines forming the angle are parallel to the superior plate of the superior vertebra and the inferior plate of the inferior vertebra. Cobb angles in the Postero-anterior and lateral views are calculated for both the thoracic and lumbar areas of the spine. Cobb angle discrepancies that are larger than  $5^\circ$  are considered as significant in clinical practice as the Cobb measurement error from radiographs has been calculated to be slightly below  $5^\circ$  [11].

Finally, in order to verify the intra-rater reproducibility of localization of the MRI landmarks, we relabeled 7 randomly chosen patients. The number of patients is chosen in order to satisfy statistical significance requirements (7 patients is equivalent to 119 vertebral bodies and 952 landmarks tested). Thus, the same 8 landmarks used for obtaining the articulated model were manually obtained a second time for each vertebra of each of the 7 patients, giving us two sets of landmarks for each patient. The reproducibility is tested in two ways : First, the Euclidean distance between the two sets of landmarks is calculated. Second, in order to test the effect of landmark localization variability on the calculation of the vertebral transformations, we calculate, for each of the 17 vertebrae, the Euclidean distance between the centroids obtained using each of the two sets of landmarks. The norm of the difference between the MRI global transformations obtained using each of

the two sets of landmarks is also calculated for each vertebra. Mean and standard deviation values are presented.

### Average spine shape model

In order to assess the shape of the spine in supine and standing postures, average Cobb angles are calculated separately for the thoracic and lumbar portions of the spine. Angles obtained from the supine posture are compared to those obtained from the standing posture in order to assess whether significant differences in curvature occur between the two postures. To this end, paired T-tests are calculated between the Cobb angles of standing and supine postures, with statistical significance differences in posture set at  $p < 0.05$ . Larger angle discrepancies between both modalities are indicative of bigger curvature changes of the spine between the two postures (when the patient is lying down (MRI) as opposed to standing up (X-ray)).

Furthermore, the variability of the spine shape is obtained using statistics on the position and the orientation of the vertebrae. We would like to define spine shapes using a common model. This would allow us to better compare patients or groups of patients. Boisvert et al. [73] presented a method to create statistical shape models built from articulated spine shapes in order to analyze deformations of the spine resulting from orthopaedic treatments. These statistical models are used in our case in order to analyze the shape of the spine obtained from X-ray and MRI data using rigid and articulated model registration. This non-quantitative assessment allows us to visualize the difference in the shape of the spine in supine and standing postures for every vertebra, and to see the effects of registration on compensating for postural differences. The spine shape model along with the average Cobb angles provide more insights on postural compensation for both registration and surgical planning.

The variability of the spine shapes is evaluated by calculating an average spine shape for each of the two postures : Standing and supine. First, for each patient, an absolute representation of each vertebra is obtained as a position and an orientation relative to the world coordinate system. This is done for each of the postures using the idea of composition of the intervertebral transformations, represented by transformation matrices, as described in section 4.4.2. The representation of transformations is then obtained as a rotation matrix  $R$  and a translation vector  $t$  ( $T = \{R, t\}$ ). Since conventional statistics don't apply on vectors, and rigid transformation belong to a Riemannian manifold, the average representation of each of the vertebral levels of the X-ray (standing) and MRI (supine) data are obtained using a generalization of the mean called the Fréchet mean  $\mu$ . For a given distance, the Fréchet mean is defined as the element of a Riemannian manifold  $M$  that minimizes the sum of the distances  $d$  with a set of elements  $x_0 \dots x_N$  of the same manifold [?] :

$$\mu = \operatorname{argmin}_{x \in M} \sum_{i=0}^N d(x, x_i)^2 \quad (4.3)$$

The mean spine shape deformations between the two postures are observed by looking at the differences between the X-ray (standing) and MRI (supine) average models.

## 4.5 Results

This section will first show quantitative results in terms of target registration error (TRE) and Cobb angle discrepancies of the registered spine between MRI and X-ray using rigid and articulated model registration. Intra-rater variability of the MRI landmark localization is also presented. Following that, the resulting average spine model will be shown.

### 4.5.1 Registration results

Table 4.1 shows the quantitative target registration error in *mm* for this study. A significant decrease in the registration error can be seen for each of the 14 patients used in this study when our proposed method is used compared to rigid registration. The results are then assessed for the thoracic and lumbar areas separately. When compared with rigid registration, the target registration error upon use of the proposed method is decreased from  $10.75 \pm 4.20\text{mm}$  to  $4.17 \pm 1.03\text{mm}$  overall, from  $9.32 \pm 3.58\text{mm}$  to  $3.91 \pm 0.94\text{mm}$  in the thoracic area, and from  $13.98 \pm 6.39\text{mm}$  to  $4.80 \pm 1.60\text{mm}$  in the lumbar area of the spine. Registration errors are generally higher in the lumbar area for all patients. Our method also has the advantage of being fast : The vertebral transformations are calculated in  $1.585 \pm 0.081$  seconds per patient using Matlab on an Intel Core i5 machine (average of 5 runs per patient for 7 patients).

Figure 4.3 reports on thoracic and lumbar Cobb angles calculated in lateral view on X-ray and registered MRI data. For both areas of the spine, the Cobb angles calculated on MRIs registered using our proposed articulated model method are nearly identical to X-ray angles. This is not the case when X-ray and rigidly registered MRIs are compared, where Cobb angles differ considerably. The mean Cobb angle discrepancy between the X-rays and the rigidly registered MRIs is  $11.98 \pm 8.65^\circ$  in the thoracic area and  $20.31 \pm 13.61^\circ$  in the lumbar area, whereas the differences between the xrays and the MRI registered with the articulated model are  $0.06 \pm 0.23^\circ$  in the thoracic area and  $0.04 \pm 0.14^\circ$  in the lumbar area. These discrepancies for the proposed method are considerably below  $5^\circ$ , an error value deemed acceptable in clinical settings as mentioned in section 4.4.3.

Similar results have been found in postero-anterior view (Figure 4.4) : The mean Cobb angle discrepancy between the X-rays and the rigidly registered MRIs is  $14.03 \pm 18.4^\circ$  in the thoracic area and  $11.38 \pm 8.79^\circ$  in the lumbar area, whereas the differences between the xrays and the MRI

Tableau 4.1 Target registration errors in mm for rigid registration and for the proposed articulated model registration (articulated).

Case	Overall rigid	Overall articulated	thoracic rigid	thoracic articulated	lumbar rigid	lumbar articulated
01	9.04	4.60	8.03	3.95	11.46	6.17
02	8.12	3.17	6.54	3.00	11.91	3.58
03	13.63	4.63	12.79	4.81	15.63	4.20
04	4.45	2.52	3.78	2.30	6.09	3.07
05	6.42	4.22	5.40	4.07	8.84	4.57
06	8.30	5.52	6.34	4.47	13.00	8.05
07	9.86	5.88	8.83	5.05	12.30	7.88
08	11.32	3.90	10.37	3.66	13.6	4.49
09	15.49	5.19	13.7	4.80	19.78	6.12
10	8.48	3.75	7.99	3.49	9.64	4.39
11	10.09	4.42	7.98	4.71	5.14	3.72
12	10.89	4.25	9.94	4.38	13.18	3.95
13	21.73	2.24	17.49	1.97	31.88	2.86
14	10.98	4.53	10.00	4.09	13.33	5.58
mean	10.75	4.17	9.31	3.90	13.41	4.80

registered with the articulated model are  $0.02 \pm 0.08^\circ$  in the thoracic area and  $0.07 \pm 0.19^\circ$  in the lumbar area.

Table 4.2 presents the landmark localization variability obtained for 7 of the 14 patients. The average difference in localization between the two sets of manual labels is of  $3.17 \pm 3.3mm$ . This difference is lower than the registration error using the articulated model; though the standard deviation is considerably higher. The variability is decreased when the vertebral centroids are calculated from the two sets of landmarks. The average distance between each of the centroids of the two sets of landmarks is  $1.57 \pm 1.13mm$ . This value is important as the centroids are used instead of the individual landmarks for the articulated model registration. The average norm of the difference in vertebral transformations is  $2.12 \pm 0.98$ . A norm of 1 signifies that the identity matrix is obtained.

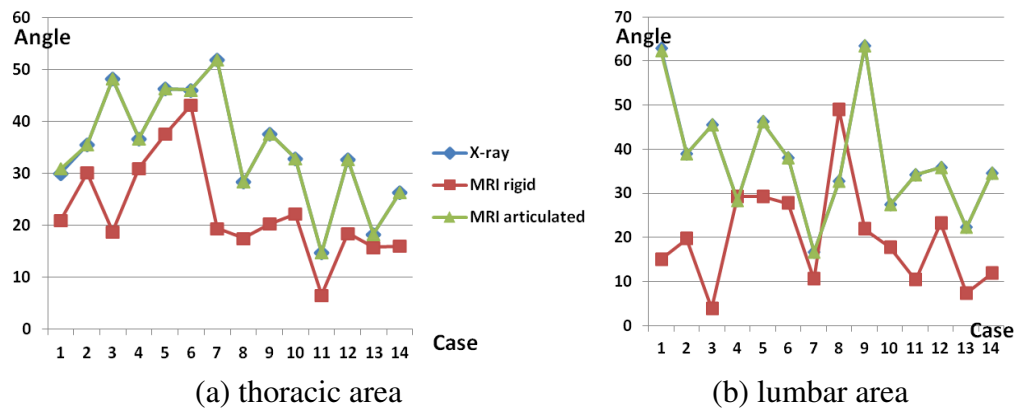


Figure 4.3 Cobb angles calculated in lateral view on thoracic and lumbar areas of the spine for the X-ray, rigidly registered MRI (MRI rigid), and MRI registered using the proposed articulated model method (MRI articulated). The average values for the thoracic area are  $34.67^\circ$ ,  $22.68^\circ$  and  $34.74^\circ$  for the X-ray, MRI rigid, and MRI articulated registrations, respectively. The average values for the lumbar area are  $37.60^\circ$ ,  $19.73^\circ$  and  $37.56^\circ$  for the X-ray, MRI rigid, and MRI articulated registrations, respectively.

Tableau 4.2 Landmark localization variability (Euclidian distance in mm) for each of seven patients tested. The variability of the vertebral centroids obtained from each set of landmarks is also shown (Average variability for the 17 vertebrae per patient). The norm of the difference in resulting vertebral transformations is also presented. (Average norm for the 17 vertebrae per patient).

Case	landmark Euclidian distance	centroid Euclidian distance	norm of transformation difference
01	3.95	2.01	2.45
02	3.14	1.42	1.95
04	2.07	0.94	1.59
06	4.38	1.44	2.00
08	3.76	2.63	3.07
10	2.18	1.44	1.99
13	2.7	1.14	1.77
mean	3.17	1.57	2.12

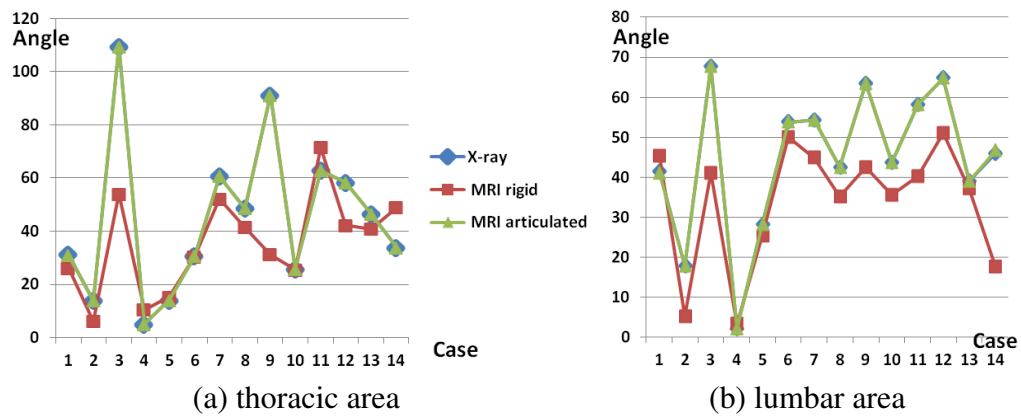


Figure 4.4 Cobb angles calculated in postero-anterior view on thoracic and lumbar areas of the spine for the X-ray, rigidly registered MRI (MRI rigid), and MRI registered using the proposed articulated model method (MRI articulated). The average values for the thoracic area are  $45.99^\circ$ ,  $35.43^\circ$  and  $45.14^\circ$  for the X-ray, MRI rigid, and MRI articulated registrations, respectively. The average values for the lumbar area are  $44.51^\circ$ ,  $33.85^\circ$  and  $44.53^\circ$  for the X-ray, MRI rigid, and MRI articulated registrations, respectively.

#### 4.5.2 Average spine shape model

The Cobb angles presented for both the postero-anterior and the lateral view in both the thoracic and lumbar areas are generally smaller in prone position as opposed to standing position ; which agrees with the hypothesis that the spine's curvature is less prominent when the patient is lying down. In the lateral view, for the thoracic area, the average Cobb angle is  $22.68^\circ$  in prone position and  $34.67^\circ$  in standing position. For the lumbar area in the same view, the average Cobb angle is  $19.73^\circ$  in prone position and  $37.60^\circ$  in standing position. Paired T-tests show statistical significance between the Cobb angles of both postures in postero-anterior view ( $p < 0.01$  for the thoracic and  $p < 0.01$  for the lumbar areas).

Similar results are obtained in the postero-anterior view : the average Cobb angle is  $35.43^\circ$  in prone position and  $45.16^\circ$  in standing position. For the lumbar area in the same view, the average Cobb angle is  $33.84^\circ$  in prone position and  $44.53^\circ$  in standing position. Paired T-tests for the postero-anterior view show a statistically significant difference between the Cobb angles of the lumbar area ( $p < 0.01$ ) but no significant difference in the thoracic area( $p = 0.05$ ).

Figure A.3 shows the average (mean) axis for each of the thoracic and lumbar levels for the X-ray and MRI vertebrae using rigid and articulated model registration. Note that since only one global rigid transformation is applied for the whole spine in the case of rigid registration, the shapes of the pre-registered and rigidly registered MRI spines are inherently identical. Thus, only the rigidly-registered average MRI spine was displayed. The average rigidly-registered MRI and X-ray axis appear to be different. However, the X-ray and articulated model registered MRI axes show a lot of similarity. This visual assessment also shows that the spine seems to be less curved in prone position (position in which the MRI was acquired), with both lumbar and thoracic curvatures being smaller when compared to the average model computed in standing position. The results in this section confirm previous claims that the curvature of the spine is generally smaller when the patient is lying down. They also confirm that the shape of the spine is significantly different in both postures, and that the articulated model presented here can be used to compensate for these differences, whether during MRI/X-ray registration or surgical planning.

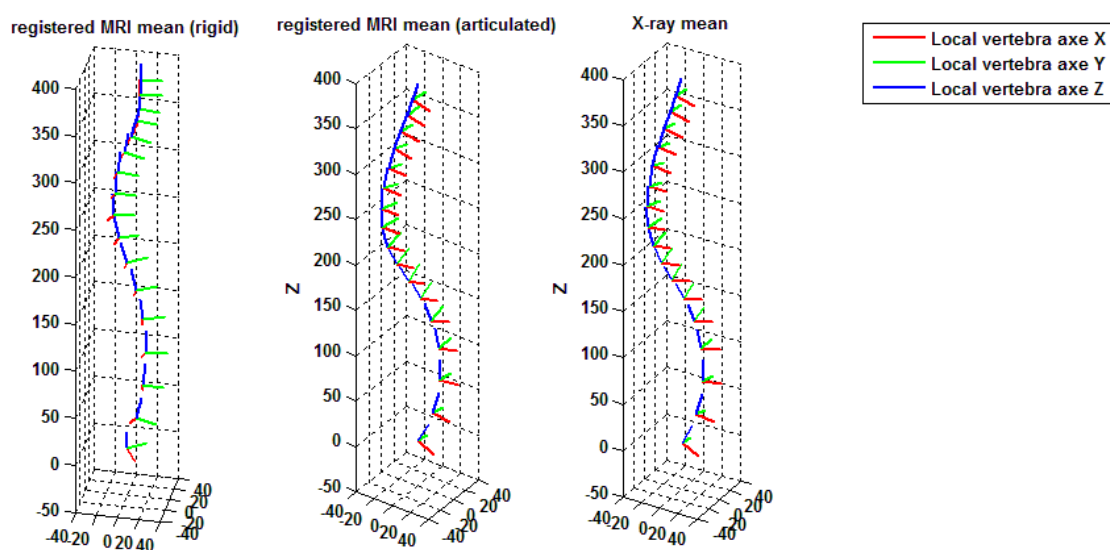


Figure 4.5 Mean vertebral axis for the rigidly registered MRI (left), the MRI registered using the articulated model (middle), and the X-ray data (right) for the 14 patients. Lumbar and thoracic vertebrae are considered in this study.



## 4.6 Discussion and conclusions

This paper described a closed form solution for the registration of two 3D reconstructions of the spine of patients with scoliosis - one obtained from X-ray images and the other one obtained from MR images - in order to compensate for spine shape differences between standing and prone postures. The proposed method uses an articulated model consisting of a series of rigid transformations, taking into account inter-vertebral transformations and thus providing a more accurate representation of the movement of the vertebral column when compared to rigid registration. The method also takes into account bone rigidity providing a more realistic deformation model when compared to non-rigid registration techniques.

Results show a decrease in the overall target registration error and a better Cobb angle correspondence when using the proposed method compared to simple rigid registration, and no significant difference in error between the thoracic and the lumbar area. Also, The Cobb angle errors obtained using our method were below the clinically accepted 5 degrees. These angles were generally smaller when the patient is lying down, proving the hypothesis that the spine loses its curvature in that position. Visual inspection of the mean shape of the spine in the 2 postures also shows that the spine has a higher curvature in standing position, and that the curvature difference is rectified following registration using the proposed method.

Since the landmark extraction is done in most part manually and the extraction process is different in the two modalities, landmark localization errors are to be expected. In the case of the X-ray reconstruction, the localization error has been previously calculated to be around  $2.1 \pm 1.5mm$  [38]. We have calculated the landmark localization intra-rater variability in the case of the MRIs to  $3.17 \pm 3.3mm$ . It should be noted though that the localization error is mitigated by an averaging done when calculating centroids. This was demonstrated as the average variability decreased to  $1.57 \pm 1.13mm$  when centroids were used instead of landmarks. The automation of landmark extraction would greatly improve the multimodal registration in addition to increasing consistency and reproducibility. We plan to use readily available automated methods in the future for the segmentation of the vertebrae and the extraction of landmarks. Those methods have been developed by Chevrefils et al. and Kadoury et al [118, 119] for the MRI and X-ray vertebrae, respectively. We also plan to eliminate the need for landmark localization in our registration framework, as our method allows for the use of higher order primitives (such as the use vertebral bodies themselves) in order to calculate the center and direction of each vertebra.

The registration of the spine serves as a preliminary step towards the construction of a geometric model of the torso of patients with scoliosis combining musculo-skeletal information along with the surface topography of the torso. In order to account for the postural change, vertebral structures will be used to register each MRI slice using the articulated model developed in this work. The

soft tissue will be confined to the volume delimited by the trunk and bone surfaces using non-rigid registration techniques, with the articulated model as an initial registration step. A patient-specific model can be obtained by registering MRI of the generic model to the X-ray and TP data of the specific patient using the same techniques as for the generic model. The resulting 3D model can then be incorporated into the simulator that is currently under development. The physical properties of the soft tissues can then be obtained and used in order to propagate the surgical correction from the spine onto the external surface of the patient's trunk. This would allow further studies in treatment techniques which would best benefit patients and improve their quality of life. Little work has been done in this field so far, and no other method registers MRI to X-ray data that can be acquired in a clinical setting. The present framework will allow us to compensate for the changes in spinal shape when building the full body model in standing position.

## RÉFÉRENCES

- [1] B. Zitova et J. Flusser, “Image registration methods : A survey,” *Image and Vision Computing*, vol. 21, no. 11, pp. 977 – 1000, 2003.
- [2] J. Cottalorda et R. Kohler, “Recueil terminologique de la scoliose idiopathique,” in *La scoliose idiopathique (sous la direction de J. Bérard et R. Kohler)* (S. Médical, ed.), pp. 33–40, 1997.
- [3] M. Asher, G. Beringer, J. Orrick et N. Halverhout, “The current status of scoliosis screening in north america, 1986 : Results of a survey by mailed questionnaire.,” *Spine*, vol. 14, pp. 652–662, 1989.
- [4] J. Roach, “Adolescent idiopathic scoliosis,” *Orthop Clin North Am.*, vol. 30, pp. 353–365, 1999.
- [5] C. Goldberg, M. Kaliszer, D. Moore, E. Fogarty et F. Dowling, “Surface topography, Cobb angles, and cosmetic change in scoliosis.,” *Spine*, vol. 26, no. 4, pp. E55–63, 2001.
- [6] V. Pazos, F. Cheriet, J. Dansereau et H. Labelle, “Quantitative analysis of external trunk asymmetry pre and post surgery comparison,” in *35e réunion annuelle de la Société de Scoliose du Québec*, 2005.
- [7] O. Dionne, “Développement d’un modèle numérique simplifié du tronc pour simulate l’effet d’une chirurgie de la scoliose sur l’apparence externe d’un patient,” Master’s thesis, École Polytechnique, Montreal, Canada, 2009.
- [8] O. Dionne, K. C. Assi, S. Grenier, H. Labelle, F. Guibault et F. Cheriet, “Simulation of the postoperative trunk appearance in scoliosis surgery,” in *to appear in : International Symposium on Biomedical Imaging (ISBI)*, (Newark, NJ), IEEE, 2012.
- [9] J. Clin, *Etude biomecanique du traitement de la scoliose idiopathique par orthese : Effets des parametres de conception des corsets sur les corrections geometriques et sur les contraintes internes du rachis*. Thse de Doctorat, École Polytechnique, Montréal, Canada, 2010.
- [10] A. F. Stokes, “Three-dimensional terminology of spinal deformity : a report presented to the scoliosis research society by the scoliosis research society working group on 3-d terminology of spinal deformity,” *Spine*, vol. 19, no. 2, pp. 236–248, 1994.
- [11] R. Morrissy, G. Goldsmith, E. Hall, D. Kehl et G. Cowie, “Measurement of the cobb angle on radiographs of patients who have scoliosis. evaluation of intrinsic error.,” *Journal of Bone and Joint Surgery*, vol. 72A, no. 3, pp. 320 –327, 1990.

- [12] L. Seoud, *Analyse de la relation entre les déformations scoliotiques du tronc et celles des structures osseuses sous-jacentes*. Thse de Doctorat, École Polytechnique, Montreal, Canada, 2012.
- [13] A. G. Webb, *Introduction to Biomedical Imaging (IEEE Press Series on Biomedical Engineering)*. Wiley-IEEE Press, Dcembre 2002.
- [14] S. Deschênes, G. Charron, G. Beaudoin, H. Labelle, J. Dubois, M.-C. Miron et S. Parent, “Diagnostic Imaging of Spinal Deformities : Reducing Patients Radiation Dose With a New Slot-Scanning X-ray Imager,” *Spine*, 2010.
- [15] F. Cheriet, J. Dansereau, Y. Petit, C.-E. Aubin, H. Labelle et J. De Guisei, “Towards the self-calibration of a multiview radiographic imaging system for the 3d reconstruction of the human spine and rib cage,” *International Journal of Pattern Recognition and Artificial Intelligence*, vol. 13, no. 5, pp. 761–79, 1999.
- [16] Q. H. Liao, “Fusion of deformable anatomical structures of human torso,” Master’s thesis, École Polytechnique, Montreal (Canada), 2005.
- [17] F. Miled, *Analyse de la géométrie externe du tronc scoliotique en flexion latérale*. M.sc.a., Ecole Polytechnique, Montreal (Canada), 2007. relevant - have.
- [18] N. SHAWAFATY, “Évaluation non invasive de leffet du traitement par corset SpineCor sur la géométrie externe du tronc,” Master’s thesis, École Polytechnique, Montréal, Canada, 2007.
- [19] N. Chihab, “Vers une mÉthode automatique de reconstruction 3D du tronc scoliotique,” Master’s thesis, École Polytechnique, Montréal, Canada, 2012.
- [20] J. V. Hajnal, *Medical Image Registration (Biomedical Engineering)*. CRC Press, Cambridge, 1 ed., Juin 2001.
- [21] A. Barton, “The regulation of mobile health applications,” *BMC Medicine*, vol. 10, pp. 46+, Mai 2012.
- [22] M. Pop, C. Duncan, G. Barequet, M. Goodrich, W. Huang et S. Kumar, “Efficient perspective-accurate silhouette computation and applications,” in *Proceedings of the Annual Symposium on Computational Geometry*, pp. 60–68, 2001.
- [23] H. Sundar, D. Silver, N. Gagvani et S. Dickinson, “Skeleton based shape matching and retrieval,” in *Shape Modeling International*, pp. 130–139, 2003.
- [24] P. Beaudet, “Rotationally invariant image operator,” in *Proc. Intl. Joint Conf. on Pattern Recognition*, pp. 579–583, 1978.
- [25] M. Harris, C. andS tephens, “A combined corner and edge detector,” in *Alvey Vision Conference*, p. 147152, 1988.

- [26] D. G. Lowe, "Object recognition from local scale-invariant features," in *International Conference on Computer Vision*, (Corfu, Greece), pp. 1150–1157, 1999),.
- [27] P. J. Besl et N. D. McKay, "A method for registration of 3-D shapes," *IEEE Trans. Pat. Anal. and Mach. Intel.*, vol. 14, no. 2, pp. 239–256, 1992.
- [28] B. H. Okker, C. H. Yan, J. Zhang, S. H. Ong et S. H. Teoh, "Accurate and fully automatic 3d registration of spinal images using normalized mutual information," in *2004 IEEE International Workshop on Biomedical Circuits and Systems*, (Singapore), pp. S3/1–5–8, IEEE, 2004.
- [29] van de Kraats EB, van Walsum T, V. JJ, O. FC, V. MA et N. WJ., "Noninvasive magnetic resonance to three-dimensional rotational x-ray registration of vertebral bodies for image-guided spine surgery," *Spine*, vol. 29, no. 3, pp. 293–7, 2004.
- [30] H. Yangqiu, S. K. Mirza, J. G. Jarvik, P. J. Heagerty et D. R. Haynor, "MR and CT image fusion of the cervical spine : a noninvasive alternative to CT-myelography," in *Medical Imaging 2005 : Visualization, Image-Guided Procedures, and Display*, vol. 5744 of *Proceedings of the SPIE - The International Society for Optical Engineering*, (San Diego, CA), pp. 481–91, SPIE-Int. Soc. Opt. Eng, 2005.
- [31] G. Champleboux, S. Lavallee, R. Szeliski et L. Brunie, "From accurate range imaging sensor calibration to accurate model-based 3d object localization," in *Proceedings. IEEE Computer Society Conference on Computer Vision and Pattern Recognition*, pp. 83–9, 1992.
- [32] W. W. III, P. Viola, H. Atsumi, S. Nakajima et R. Kikinis, "Multi-modal volume registration by maximization of mutual information," *Med Image Anal*, vol. 1, pp. 35–51, 03 1996.
- [33] T. M. Buzug, J. Weese et C. Lorenz, "Weighted least squares for point-based registration in digital subtraction angiography (dsa)," in *Proc. SPIE* (K. M. Hanson, ed.), vol. 3661 of *Society of Photo-Optical Instrumentation Engineers (SPIE) Conference*, pp. 139–150, May 1999.
- [34] E. van de Kraats, T. van Walsum, J. Verlaan, F. Oner, M. Viergever et W. Niessen, "Noninvasive Magnetic Resonance to Three-Dimensional Rotational X-Ray Registration of Vertebral Bodies for Image-Guided Spine Surgery," *Spine*, vol. 29, no. 3, pp. 293–297, 2004.
- [35] D. Tomazevic, B. Likar et F. Pernus, "3-D/2-D registration by integrating 2-D information in 3-D," *IEEE Transactions on Medical Imaging*, vol. 25, no. 1, pp. 17–27, 2006.
- [36] E. B. van de Kraats, G. P. Penney, D. Tomazevic, T. van Walsum et W. J. Niessen, "Standardized evaluation methodology for 2-D-3-D registration," *IEEE Transactions on Medical Imaging*, vol. 24, no. 9, pp. 1177–89, 2005.

- [37] Z. Tang et J. Pauli, "Fully automatic extraction of human spine curve from MR images using methods of efficient intervertebral disk extraction and vertebra registration," *Int J CARS*, vol. 6, no. 1, pp. 21–33, 2011.
- [38] S. Delorme, H. Labelle, B. Poitras, C.-H. Rivard, C. Coillard et J. Dansereau, "Pre-, intra-, and postoperative three-dimensional evaluation of adolescent idiopathic scoliosis.," *Journal of spinal disorders*, vol. 13, no. 2, pp. 93–101, 2000.
- [39] F. Bookstein, "Principal warps : thin-plate splines and the decomposition of deformations.," *Pattern Analysis and Machine Intelligence, IEEE Transactions on*, vol. 11, no. 6, pp. 567 – 585, 1989.
- [40] K. Rohr, H. Stiehl, T. Sprengel, R. and Buzug, J. Weese et M. Kuhn, "Landmark-based elastic registration using approximating thin-plate splines," *IEEE Transactions on Medical Imaging*, vol. 20, no. 6, pp. 526–534, 2001.
- [41] J. A. Little, D. L. G. Hill et D. J. Hawkes, "Deformations incorporating rigid structures," in *Proceedings of the Workshop on Mathematical Methods in Biomedical Image Analysis*, (San Francisco, CA), pp. 104–13, IEEE Comput. Soc. Press, 1996.
- [42] K. Rohr, M. Fornefett et S. Siegfried, "Approximating thin-plate splines for elastic registration : Integration of landmark errors and orientation attributes.," *Lecture Notes in Computer Science*, vol. 1613, pp. 252–265, 1999.
- [43] R. H. Huesman, G. J. Klein, J. A. Kimdon, C. Kuo et S. Majumdar, "Deformable registration of multimodal data including rigid structures," *IEEE Transactions on Nuclear Science*, vol. 50, no. 3, pp. 389–92, 2003.
- [44] D. Loeckx, F. Maes, D. Vandermeulen et P. Suetens, "Nonrigid image registration using free-form deformations with a local rigidity constraint," in *Medical Image Computing and Computer-Assisted Intervention - MICCAI 2002. 5th International Conference. Proceedings Part II*, pp. 461–8, Springer-Verlag, 2004.
- [45] H. J. Johnson et G. E. Christensen, "Landmark and intensity-based, consistent thin-plate spline image registration," in *Proceedings of the 17th International Conference on Information Processing in Medical Imaging, IPMI '01*, (London, UK, UK), pp. 329–343, Springer-Verlag, 2001.
- [46] M. Davis, A. Khotanzad, D. Flamig et S. Harms, "A physics-based coordinate transformation for 3-d image matching.," *IEEE Transactions on Medical Imaging*, vol. 16, no. 3, pp. 317–328, 1988.
- [47] Z. Xie et G. Farin, "Image registration using hierarchical b-splines," *Visualization and Computer Graphics, IEEE Transactions on*, vol. 10, no. 1, pp. 85– 94, 2004.

- [48] S. Aschkenasy, C. Jansen, R. Osterwalder, A. Linka, M. Unser, S. Marsch et P. Hunziker, “Unsupervised image classification of medical ultrasound data by multiresolution elastic registration,” *Ultrasound in Medicine & Biology*, vol. 32, no. 1047, 2006.
- [49] D. Rueckert, L. I. Sonoda, C. Hayes, M. Hill, D. L. G. Leach et D. J. Hawkes, “Nonrigid registration using free-form deformations : Application to breast MR images,” *IEEE Trans. Med. Imag.*, vol. 18, pp. 712–721, 1999.
- [50] J. A. Schnabel, D. Rueckert, M. Quist, J. M. Blackall, A. D. Castellano-Smith, T. Hartkens, G. P. Penney, W. A. Hall, H. Liu, C. L. Truwit, F. A. Gerritsen, D. L. G. Hill et D. J. Hawkes, “A generic framework for non-rigid registration based on non-uniform multi-level free-form deformations,” in *Proceedings of the 4th International Conference on Medical Image Computing and Computer-Assisted Intervention, MICCAI '01*, (London, UK, UK), pp. 573–581, Springer-Verlag, 2001.
- [51] J. M. Blackall, G. P. Penney, A. P. King et D. J. Hawkes, “Alignment of sparse freehand 3-D ultrasound with preoperative images of the liver using models of respiratory motion and deformation,” *IEEE transactions on medical imaging*, vol. 24, no. 11, pp. 1405–1416, 2005.
- [52] R. Szeliski et S. Lavalée, “Matching 3-d anatomical surfaces with non-rigid deformations using octree-splines,” *International Journal of Computer Vision*, vol. 18, no. 2, pp. 171–86, 1996.
- [53] Y. Yuhui, A. Bull, D. Rueckert et A. Hill, “3D statistical shape modelling of long bones,” in *Third International Workshop on Biomedical Image Registration (WBIR 2006)*, 2006.
- [54] D. Skerl, B. Likar et F. Pernus, “Evaluation of similarity measures for non-rigid registration,” in *Biomedical Image Registration. Third International Workshop, WBIR 2006. Proceedings*, (Utrecht, Netherlands), pp. 160–8, Springer-Verlag, 2006.
- [55] K. Wang, Y. He et H. Qin, “Incorporating rigid structures in non-rigid registration using triangular b-splines,” in *Variational, geometric and level set methods in computer vision (VLSM)*, pp. 235–246, 2005.
- [56] M. Staring, S. Klein et J. Pluim, “Nonrigid Registration Using a Rigidity Constraint,” in *SPIE Medical Imaging : Image Processing* (J. Reinhardt et J. Pluim, eds.), vol. 6144 of *Proceedings of SPIE*, (San Diego, California, USA), pp. 614413–1 – 614413–10, SPIE press, février 2006.
- [57] D. R. J. A. F. M. R. J. B. M. Kessler, “Nonrigid registration using regularization that accommodates local tissue rigidity,” in *Proc. SPIE*, vol. 6144, 2006.
- [58] J. V. Miller, G. Gopalakrishnan, M. Datar, P. R. S. Mendonca et R. Mullick, “Deformable registration with spatially varying degrees of freedom constraints,” pp. 1163–1166, Juin 2008.

- [59] N. Chihab, *Optimal Registration of Deformed Images NAJAT CHIHAB*. Thse de Doctorat, Computer and Information Science Dept., University of Pennsylvania, Philadelphia, PA, 1981.
- [60] R. Bajcsy et S. Kovacic, "Multiresolution elastic matching," *Computer Vision, Graphics, and Image Processing*, vol. 46, no. 1, pp. 1 – 21, 1989.
- [61] J. C. Gee, D. R. Haynor, L. L. Briquer et R. Bajcsy, "Advances in elastic matching theory and its implementation," in *Proceedings of the First Joint Conference on Computer Vision, Virtual Reality and Robotics in Medicine and Medial Robotics and Computer-Assisted Surgery*, CVRMed-MRCAS '97, (London, UK, UK), pp. 63–72, Springer-Verlag, 1997.
- [62] D. C. Alexander, J. C. Gee et R. Bajcsy, "Transformations of and similarity measures for diffusion tensor MRI's," 1999.
- [63] G. Christensen, M. Miller et M. Vannier, "'a 3d deformable magnetic resonance textbook based on elasticity," in *Proc. AAAI Workshop : Application of Computer Vision in Medical Image Processing*, pp. 153–156, 1994.
- [64] G. E. Christensen, R. D. Rabbitt et M. I. Miller, "3d brain mapping using a deformable neuroanatomy," *Physics in Medicine and Biology*, vol. 39, no. 3, p. 609, 1994.
- [65] M. Bro-Nielsen et C. Gramkow, "Fast fluid registration of medical images," in *SPIE Visualization in Biomedical Computing* (K. Hone et R. Kikinis, eds.), vol. 1131, pp. 267–276, Incs, 1996.
- [66] E. D'Agostino, F. Maes, D. Vandermeulen et P. Suetens, "A viscous fluid model for multimodal non-rigid image registration using mutual information," *Medical Image Analysis*, vol. 7, no. 4, pp. 565 – 575, 2003.
- [67] S. Tang et T. Jiang, "Fast non-rigid medical image registration by fluid model," in *Asian Conference on Computer Vision*, pp. 27–30, 2004.
- [68] K. Saddi, *RECALAGE NON RIGIDE ET SEGMENTATION AUTOMATIQUE DIMAGES DE PERFUSION DU FOIE*. Thse de Doctorat, École Polytechnique, Montreal, Canada, 2008.
- [69] B. Glocker, N. Komodakis, N. Paragios et N. Navab, "Non-rigid Registration using Discrete MRFs : Application to Thoracic CT Images," in *Workshop Evaluation of Methods for Pulmonary Image Registration in conjunction with Medical Image Computing and Computer-Assisted Intervention*, 2010.
- [70] D. Mahapatra et Y. Sun, "Nonrigid registration of dynamic renal mr images using a saliency based mrf model," in *Proceedings of the 11th international conference on Medical Image Computing and Computer-Assisted Intervention - Part I, MICCAI '08*, (Berlin, Heidelberg), pp. 771–779, Springer-Verlag, 2008.



- [71] T. W. H. Tang et A. C. S. Chung, “Non-rigid image registration using graph-cuts,” in *Proceedings of the 10th international conference on Medical image computing and computer-assisted intervention - Volume Part I, MICCAI’07*, (Berlin, Heidelberg), pp. 916–924, Springer-Verlag, 2007.
- [72] R. W. K. So, T. W. H. Tang et A. C. S. Chung, “Non-rigid image registration of brain magnetic resonance images using graph-cuts,” *Pattern Recogn.*, vol. 44, pp. 2450–2467, Octobre 2011.
- [73] J. Boisvert, X. Pennec, H. Labelle, F. Cheriet et N. Ayache, “Principal spine shape deformation modes using riemannian geometry and articulated models,” in *Articulated Motion and Deformable Objects. 4th International Conference, AMDO. Proceedings* (L. N. i. C. Science, ed.), vol. 4069, pp. 346–55, 2006.
- [74] J. Boisvert, X. Pennec, N. Ayache, H. Labelle et K. Cheriet, “3d anatomical variability assessment of the scoliotic spine using statistics on lie groups,” in *2006 3rd IEEE International Symposium on Biomedical Imaging : Macro to Nano*, (Arlington, VA), pp. 750–3, IEEE, 2006.
- [75] D. C. Moura, J. Boisvert, J. G. Barbosa et J. M. R. S. Tavares, “Fast 3d reconstruction of the spine using user-defined splines and a statistical articulated model,” in *ISVC (1)* (G. Bebis, R. D. Boyle, B. Parvin, D. Koracin, Y. Kuno, J. Wang, R. Pajarola, P. Lindstrom, A. Hinkenjann, M. L. Encarnação, C. T. Silva et D. S. Coming, eds.), vol. 5875 of *Lecture Notes in Computer Science*, pp. 586–595, Springer, 2009.
- [76] S. Kadoury et N. Paragios, “Surface/volume-based articulated 3D spine inference through markov random fields,” in *MICCAI*, pp. 92–99, 2009.
- [77] S. N. Le, J. Karlekar et A. C. Fang, “Articulated registration of 3d human geometry to x-ray image,” in *ICIP*, pp. 1108–1111, IEEE, 2008.
- [78] T. Klinder, J. Ostermann, M. Ehm, A. Franz, R. Kneser et C. Lorenz, “Automated model-based vertebra detection, identification, and segmentation in ct images,” *Medical Image Analysis*, vol. 13, no. 3, pp. 471 – 482, 2009.
- [79] A. du Bois d’Aische, M. De Craene, B. Macq et S. Warfield, “An improved articulated registration method for neck images.” in *Conf Proc IEEE Eng Med Biol Soc*, pp. 7668–71, 2005.
- [80] S. Gill, P. Abolmaesumi, G. Fichtinger, J. Boisvert, D. Pichora, D. Borshneck et P. Mousavi, “Biomechanically constrained groupwise ultrasound to ct registration of the lumbar spine,” *Medical Image Analysis*, vol. 16, no. 3, pp. 662 – 674, 2012.
- [81] L. R. Dice, “Measures of the amount of ecologic association between species,” *Ecology*, vol. 26, no. 3, pp. 1037–1044, 1945.

- [82] A. P. Zijdenbos, B. M. Dawant, R. A. Margolin et A. C. Palmer, “Morphometric analysis of white matter lesions in mr images : method and validation.” *IEEE Transactions on Medical Imaging*, vol. 13, no. 4, pp. 716–24, 1994.
- [83] L. Xia, T. E. Peterson, J. C. Gore et B. M. Dawant, “Automatic inter-subject registration of whole body images,” in *Biomedical Image Registration. Third International Workshop, WBIR 2006. Proceedings*, (Utrecht, Netherlands), pp. 18–25, Springer-Verlag, 2006.
- [84] W. Qi, L. Gu et J. Xu, “Non-rigid 2D-3D registration based on support vector regression estimated similarity metric,” in *Fourth international workshop on medical imaging and augmented reality*, vol. 5128, p. 33948, Lecture Notes in Computer Science, Springer, 2005.
- [85] L. Brunie, S. Lavallee, J. Troccaz, P. Cinquin, et M. Bolla, “Pre- and intra-irradiation multi-modal image registration : principles and first experiments, radiother.,” *Oncol.*, vol. 29, no. 2, pp. 244–252, 1993.
- [86] R. McLaughlin, J. Hipwell, D. Hawkes, J. Noble, J. Byrne et T. Cox, “A comparison of a similarity-based and a feature-based 2-D3-D registration method for neurointerventional use,” *IEEE Trans Med Imaging*, vol. 24, no. 8, p. 105866, 2005.
- [87] D. Alperin et C. Pelizzari, “Retrospective registration of x-ray angiograms with mr images by using vessels as intrinsic landmarks,” *J Magn Reson Imaging*, vol. 4, no. 2, pp. 139–44, 1994.
- [88] E. Bullitt, A. Liu, S. Aylward, C. Coffey, J. Stone, S. Mukherji, K. Muller et S. Pizer, “Registration of 3d cerebral vessels with 2d digital angiograms : clinical evaluation,” *Acad. Radiol.*, vol. 6, no. 9, pp. 539–546, 1999.
- [89] H. Chan, A. Chung, S. Yu et W. Wells, “2D3D vascular registration between digital subtraction angiographic (DSA) and magnetic resonance angiographic (MRA) images vol. 1.” in *IEEE international symposium on biomedical imaging : nano to macro*, p. p. 70811., 2004.
- [90] C. Florin, J. Williams, A. Khamene et N. Paragios, “Registration of 3D angiographic and X-ray images using sequential Monte Carlo sampling,” in *First international workshop on computer vision for biomedical image applications (CVBIA 2005)*, vol. 3765, p. 42736, Lecture Notes in Computer Science, Springer, 2005.
- [91] C. Chung<sup>1</sup>, W. M. I. Wells, A. Norbash et G. W. E. L., “Multi-modal image registration by minimising KullbackLeibler distance.” in *Fifth international conference on medical image computing and computer-assisted intervention (MICCAI 2002)* vol. 2489, p. 52532, Lecture Notes in Computer Science, Springer, 2002.
- [92] Y. Kita, D. Wilson et J. Noble, “Real-time registration of 3D cerebral vessels to Xray angiograms,” in *First international conference on medical image computing and computer-*

- assisted intervention (MICCAI-98)*, vol. 1496., p. 112533, Lecture Notes in Computer Science, Springer, 1998.
- [93] J. Hipwell, G. Penney, R. McLaughlin, K. Rhode, P. Summers, T. Cox et al., “Intensity-based 2-D/3-D registration of cerebral angiograms,” *IEEE Trans Med Imaging*, vol. 22, no. 11, p. 141726, 2003.
- [94] M. Vermandel, N. Betrouni, J. Gauvrit, D. Pasquier, C. Vasseur et J. Rousseau, “Intrinsic 2D/3D registration based on a hybrid approach : use in the radiosurgical imaging process,” *Cell Mol Biol*, vol. 52, no. 6, p. 4453, 2006.
- [95] K. Miller, A. Hebb, D. Hermes, M. den Nijs, J. Ojemann et R. Rao, “Brain surface electrode co-registration using mri and x-ray,” in *Conf Proc IEEE Eng Med Biol Soc.*, pp. 6015–8, IEEE, 2010.
- [96] S. D. Buck, F. Maes, J. Ector, J. Bogaert, S. Dymarkowski, H. Heidbuchel et P. Suetens, “An augmented reality system for patient-specific guidance of cardiac catheter ablation procedures,” *IEEE Trans. Med. Imag.*, vol. 24, no. 11, pp. 1512–1524, 2005.
- [97] J. Jomier, E. Bullitt, M. Van Horn, C. Pathak et S. Aylward, “3D/2D model-to-image registration applied to tips surgery,” in *Ninth international conference on medical image computing and computerassisted intervention (MICCAI 2006), part 2*, vol. 4191, p. 6629, Lecture Notes in Computer Science, Springer, 2006.
- [98] K. Rhode, D. Hill, P. Edwards, J. Hipwell, D. Rueckert, G. S. Ortiz, S. Hegde, V. Rahunathan et R. Razavi, “Registration and tracking to integrate X-ray and MR images in an XMR facility,” *IEEE Transactions on Medical Imaging*, vol. 22, no. 11, pp. 1369–78, 2003.
- [99] K. Rhode, M. Sermesant, D. Brogan, S. Hegde, J. Hipwell, P. Lambiase, E. Rosenthal, C. Bucknall, S. Qureshi, J. Gill, R. Razavi et D. Hill, “A system for real-time xmr guided cardiovascular intervention,” *IEEE Trans. Med. Imag.*, vol. 24, no. 11, pp. 1428–1440, 2005.
- [100] A. K. George, R. J. Lederman, et A. Z. Faranesh, “Robust automatic rigid registration of mri and x-ray using external fiducial markers for xfm-guided interventional procedures,” *Med. Phys.*, vol. 38, no. 125, 2011.
- [101] Y. Ma, S. Duckett, P. Chinchapatnam, G. Gao, A. Shetty, C. Rinaldi, T. Schaeffter et K. S. Rhode, “Mri to x-ray fluoroscopy overlay for guidance of cardiac resynchronization therapy procedures,” *Computers in Cardiology*, pp. 229–232, 2010.
- [102] M. Miquel, K. Rhode, P. Acher, N. MacDougall, J. Blackall, R. Gaston, S. Hegde, S. Morris, R. Beaney, C. Deehan, R. Popert et S. Keevil, “Using combined x-ray and mr imaging for prostate i-125 post-implant dosimetry : phantom validation and preliminary patient work,” *Phys. Med. Biol.*, vol. 51, no. 5, pp. 1129–1137, 2006.

- [103] T. Rohlfing et C. R. Maurer, Jr., “A novel image similarity measure for registration of 3-d mr images and x-ray projection images,” in *Proceedings of the 5th International Conference on Medical Image Computing and Computer-Assisted Intervention-Part II*, MICCAI '02, (London, UK, UK), pp. 469–476, Springer-Verlag, 2002.
- [104] G. Zheng, X. Dong et M. A. G. Ballester, “Unsupervised reconstruction of a patient-specific surface model of a proximal femur from calibrated fluoroscopic images,” in *Proceedings of the 10th international conference on Medical image computing and computer-assisted intervention - Volume Part I*, MICCAI'07, (Berlin, Heidelberg), pp. 834–841, Springer-Verlag, 2007.
- [105] S. Benameur, F. Mignotte, Destrempes et J. de Guise, “Three-dimensional biplanar reconstruction of scoliotic rib cage using the estimation of a mixture of probabilistic prior models,” *IEEE Trans. Biomed. Eng.*, vol. 52, no. 10, pp. 1713–1728, 2005.
- [106] M. J. van der Bom, J. P. W. Pluim, M. J. Gounis, E. B. van de Kraats, S. M. Sprinkhuizen, J. Timmer, R. Homan et L. W. Bartels, “Registration of 2d x-ray images to 3d mri by generating pseudo-ct data,” *Physics in Medicine and Biology*, vol. 56, no. 4, p. 1031, 2011.
- [107] T. Mertzaniidou, J. H. Hipwell, M. J. Cardoso, C. Tanner, S. Ourselin et D. J. Hawkes, “X-ray mammography ; mri registration using a volume-preserving affine transformation and an em-mrf for breast tissue classification,” in *Proceedings of the 10th international conference on Digital Mammography*, IWDM'10, (Berlin, Heidelberg), pp. 23–30, Springer-Verlag, 2010.
- [108] P. Markelj, D. Tomazevic, B. Likar et F. Pernus, “A review of 3D/2D registration methods for image-guided interventions,” *Med Image Anal*, vol. 16, no. 3, 2010.
- [109] D. Tomazevic, B. Likar et F. Pernus, “3-D/2-D registration by integrating 2-D information in 3-D,” *IEEE Transactions on Medical Imaging*, vol. 25, no. 1, pp. 1407–1416, 2003.
- [110] E. B. van de Kraats, G. P. Penney, T. van Walsum et W. J. Niessen, “Multispectral mr to x-ray registration of vertebral bodies by generating ct-like data,” in *Proceedings of the 8th international conference on Medical image computing and computer-assisted intervention - Volume Part II*, MICCAI'05, (Berlin, Heidelberg), pp. 911–918, Springer-Verlag, 2005.
- [111] P. Markelj, D. Tomazevic, F. Pernus et B. Likar, “Optimizing bone extraction in MR images for 3D/2D gradient based registration of MR and X-ray images,” in *J. Reinhardt and J. Pluim, Editors, Medical Imaging 2007 : Image Processing vol. 6512, SPIE, San Diego, CA, USA*, 2007.
- [112] P. Markelj, D. Tomazevic, F. Pernus et B. Likar, “Robust gradientbased 3-D/2-D registration of CT and MR to X-ray images,” *IEEE Transactions on Medical Imaging*, vol. 27, no. 12, 2008.

- [113] R. Harmouche, F. Cheriet, H. Labelle et J. Dansereau, “Articulated Model Registration of MRI/X-Ray Spine Data,” in *ICIAR (2)*, pp. 20–29, 2010.
- [114] B. Andre, J. Dansereau et H. Labelle, “Three- dimensional reconstruction of the human spine,” *J Biomech*, vol. 28, pp. 1023–1035, 1994.
- [115] S. Delorme, Y. Petit, C.-E. Aubin, J. Dansereau, H. Labelle, C. Landry et J. de Guise, “Three-dimensional modelling and rendering of the human skeletal trunk from 2d radiographic images,” in *International Conference on 3D Digital Imaging and Modeling, 3DIM’99*, (Los Alamitos, CA, USA), pp. 497–505, IEEE Computer Society, 1999.
- [116] B. K. P. Horn, “Closed-form solution of absolute orientation using unit quaternions,” *Journal of the Optical Society of America A*, vol. 4, no. 4, pp. 629–642, 1987.
- [117] C. JR, “Outline for the study of scoliosis.,” *Instr Course Lect.*, vol. 5, pp. 261–75, 1948.
- [118] S. Kadoury, F. Cheriet et H. Labelle, “Segmentation of scoliotic spine silhouettes from enhanced biplanar x-rays using a prior knowledge bayesian framework,” in *Proceedings of the Sixth IEEE international conference on Symposium on Biomedical Imaging : From Nano to Macro*, ISBI’09, (Piscataway, NJ, USA), pp. 478–481, IEEE Press, 2009.
- [119] C. Chevrefils, F. Cheriet, C.-E. Aubin et G. Grimard, “Texture analysis for automatic segmentation of intervertebral disks of scoliotic spines from mr images,” *IEEE Transactions on Information Technology in Biomedicine*, vol. 13, no. 4, pp. 608–620, 2009.
- [120] Y.-T. Chen et M.-S. Wang, “Three-dimensional reconstruction and fusion for multi-modality spinal images,” *Computerized Medical Imaging and Graphics*, vol. 28, no. 1-2, pp. 21–31, 2004.
- [121] R. Harmouche, F. Cheriet, H. Labelle et J. Dansereau, “3D registration of MR and X-ray spine images using an articulated model,” *Comp. Med. Imag. and Graph.*, vol. 36, no. 5, pp. 410–418, 2012.
- [122] R. H. Huesman, G. J. Klein, J. A. Kimdon, C. Kuo et S. Majumdar, “Deformable registration of multi-modal data including rigid structures,” in *2002 IEEE Nuclear Science Symposium Conference Record*, vol. 3, (Norfolk, VA), pp. 1879–82 vol.3, IEEE, 2003.
- [123] E. van de Kraats, G. Penney, T. van Walsum et W. Niessen, “Multispectral MR to X-ray registration of vertebral bodies by generating CT-like data,” in *Conference on Medical Image Computing and Computer-Assisted Intervention (MICCAI 2005), Part 2*, 2005.
- [124] M.-E. Lamarre, S. Parent, H. Labelle, C.-E. Aubin, J. Joncas, A. Cabral et Y. Petit, “Assessment of Spinal Flexibility in Adolescent Idiopathic Scoliosis : Suspension Versus Side-Bending Radiography,” *Spine*, vol. 34, pp. 591–597, 2009.

- [125] M. E. Rose, *Elementary Theory of Angular Momentum*. New York : John Wiley & Sons, 1955.